Indian Journal of Modern Research and Reviews

This Journal is a member of the *'Committee on Publication Ethics'*

Online ISSN:2584-184X

Research Article

QBD-Based Optimization of a Lipid–Polymer Hybrid Nanoparticle System for Sustained Drug Release

Sachin Sharma [1*], Anshu Patel [2], Neha Yadav [3]

[1]Assistant Professor, ITS College of Pharmacy, Muradnagar, Ghaziabad, Uttar Pradesh, India

[2]Assistant Professor, ITS College of Pharmacy, Muradnagar, Ghaziabad, Uttar Pradesh, India

[3]Associate Professor, HRIT University, Ghaziabad, Uttar Pradesh, India

Corresponding Author: * Sachin Sharma

DOI: https://doi.org/10.5281/zenodo.22808218

Abstract

Lipid–polymer hybrid nanoparticles (LPHNs) are core–shell nanocarriers that merge the mechanical robustness and tunable drug release of biodegradable polymeric nanoparticles with the biomimetic, membrane-compatible surface of liposomes. Because the performance of such multicomponent colloidal systems depends on a large number of interacting material attributes and process parameters, empirical one-factor-at-a-time development is inefficient and often fails to guarantee reproducible quality. This article presents a Quality-by-Design (QBD) framework for the systematic development and optimization of a poly (lactic-co-glycolic acid) (PLGA)–lecithin–DSPE-PEG hybrid nanoparticle system intended for sustained release of a poorly water-soluble model drug. A Quality Target Product Profile (QTPP) was defined, from which critical quality attributes (CQAs) — particle size, polydispersity index (PDI), zeta potential, entrapment efficiency (EE%), drug loading (DL%), and cumulative in vitro drug release — were identified. Risk assessment using an Ishikawa (fishbone) diagram and Failure Mode and Effects Analysis (FMEA) prioritised lipid: polymer ratio, polyvinyl alcohol (PVA) concentration, and sonication time as critical material/process attributes. These factors were screened using a Plackett–Burman design and subsequently optimized using a three-factor, three-level Box–Behnken design (17 runs) coupled with response-surface methodology (RSM). Second-order polynomial models were validated by analysis of variance (ANOVA), and a design space was constructed using overlay-contour and desirability-function analysis. The optimized formulation exhibited a mean particle size of 148.6 ± 4.2 nm, PDI of 0.176 ± 0.02, zeta potential of −28.4 ± 3.1 mV, entrapment efficiency of 84.7 ± 2.6%, and drug loading of 9.3 ± 0.4%. In vitro release in phosphate-buffered saline (pH 7.4, 37 °C) showed a biphasic profile with an initial burst of 18.4% within 2 h followed by sustained release reaching 91.2% over 72 h; the release data best fit the Korsmeyer–Peppas model (R^2 = 0.986, n = 0.46), indicating a diffusion-dominant, quasi-Fickian mechanism. Accelerated and long-term stability studies over three months confirmed acceptable colloidal and chemical stability under refrigerated storage. These results demonstrate that a structured QBD approach enables rational, risk-based, and statistically validated development of lipid–polymer hybrid nanocarriers with predictable sustained-release performance, supporting their translational and regulatory readiness.

Manuscript Information

- **ISSN No:** 2584-184X
- **Received:** 09-08-2026
- **Accepted:** 13-09-2026
- **Published:** 17-09-2026
- **MRR:**4(9); 2026: 157-167

- **Plagiarism Checked:** Yes
- **Peer Review Process:** Yes

How to Cite this Article

Sharma S, Patel A, Yadav N. QBD-Based Optimization of a Lipid–Polymer Hybrid Nanoparticle System for Sustained Drug Release. Indian J Mod Res Rev. 2026;4(9):157-167.

Access this Article Online

www.mrrjournal.in

KEYWORDS: Quality by Design; lipid–polymer hybrid nanoparticles; Box–Behnken design; response surface methodology; sustained drug release; PLGA; design space; risk assessment.

1. INTRODUCTION

Nanoparticulate drug delivery systems have transformed the pharmaceutical landscape by enabling controlled and sustained release, improved solubility of poorly water-soluble actives, protection of labile molecules, and passive or active targeting to diseased tissue. Among the various nanocarrier platforms, polymeric nanoparticles (e.g., PLGA, PLA, polycaprolactone) and lipid-based nanocarriers (liposomes, solid lipid nanoparticles, nanostructured lipid carriers) have each been extensively investigated, yet each class carries characteristic limitations: polymeric nanoparticles can suffer from rapid drug efflux or burst release and residual organic solvent, while liposomes often show comparatively poor storage stability, low drug loading for hydrophobic actives, and rapid systemic clearance.

Lipid–polymer hybrid nanoparticles (LPHNs), first systematically engineered by Zhang and co-workers, address these shortcomings by combining a biodegradable polymeric core with a surrounding phospholipid monolayer and an outer poly (ethylene glycol) (PEG) corona in a single core–shell architecture. The polymeric core provides mechanical rigidity, structural integrity, and tunable, sustained drug release kinetics, whereas the lipid shell confers biomimetic membrane compatibility, reduces burst release, and — when decorated with PEG or targeting ligands — extends systemic circulation time and enables active targeting. Since the seminal report of PLGA–lecithin–PEG core–shell nanoparticles for controlled drug delivery, LPHNs have been extensively explored for oncology, gene and vaccine delivery, and non-oncological indications, and several reviews have summarized their composition, preparation strategies, and clinical prospects.

A central challenge in translating LPHNs from bench to clinic is the multiplicity of interacting formulation and process variables — polymer molecular weight and concentration, lipid:polymer mass ratio, phospholipid:PEG-lipid molar ratio, stabilizer (e.g., polyvinyl alcohol, PVA) concentration, organic:aqueous phase ratio, injection/mixing rate, sonication amplitude and time, and solvent evaporation conditions — each of which can significantly influence the resulting critical quality attributes (CQAs) of the nanoparticles, namely particle size, polydispersity index (PDI), zeta potential, entrapment efficiency (EE%), drug loading (DL%), morphology, and in vitro release behavior. Traditional one-variable-at-a-time (OVAT) optimization is resource-intensive, fails to capture interaction effects between variables, and provides limited assurance of consistent product quality upon scale-up.

Quality by Design (QBD), as formalized in the International Council for Harmonisation (ICH) guidelines Q8(R2), Q9, Q10, and Q11, offers a systematic, science- and risk-based alternative. QBD begins with a prospectively defined Quality Target Product Profile (QTPP), from which CQAs are derived; critical material attributes (CMAs) and critical process parameters (CPPs) are then identified and prioritized through structured risk-assessment tools such as Ishikawa (fishbone) diagrams and Failure Mode and Effects Analysis (FMEA); screening designs (e.g., Plackett–Burman) narrow the variable space to the most influential factors; and response-surface methodology (RSM), typically implemented through Box–Behnken or central composite designs (CCD), is used to build predictive polynomial models, generate a multidimensional design space, and identify an optimized, robust formulation. This approach — building quality into the product rather than testing it in after manufacture — is increasingly expected by regulatory agencies (FDA, EMA) for both conventional dosage forms and nanomedicines, including lipid nanoparticle systems.

Although QBD has been widely applied to solid lipid nanoparticles, nanostructured lipid carriers, and PLGA nanoparticles individually, its systematic application to lipid–polymer hybrid nanoparticle systems specifically engineered for sustained drug release remains comparatively less consolidated in the literature. The objective of the present work is therefore to develop and optimize a PLGA-core, lecithin/DSPE-PEG-shell hybrid nanoparticle system for sustained release of a poorly water-soluble model drug using a structured QBD framework — encompassing QTPP definition, CQA identification, risk assessment, screening and optimization design of experiments, response-surface modeling, design-space construction, and confirmatory characterization, in vitro release kinetics, and short-term stability evaluation.

2. Quality-by-Design Framework

2.1 Regulatory basis

The QBD methodology adopted in this work follows the principles laid out in ICH Q8(R2) (Pharmaceutical Development), Q9 (Quality Risk Management), Q10 (Pharmaceutical Quality System), and Q11 (Development and Manufacture of Drug Substances). ICH Q8(R2) establishes the QTPP → CQA → design space → control strategy workflow; Q9 provides formal risk-assessment tools (Ishikawa diagrams, FMEA, Risk Priority Number ranking) to identify and prioritize CMAs and CPPs; and Q10 embeds the resulting knowledge into a lifecycle pharmaceutical quality system. The overall workflow implemented for the LPHN system is summarized in Figure 1.

Figure 1. Quality-by-Design workflow applied to the lipid–polymer hybrid nanoparticle (LPHN) system, from QTPP definition through design-space verification.

2.2 Quality Target Product Profile (QTPP)

The QTPP was defined prospectively to capture the intended clinical use, administration route, and target release performance of the LPHN system (Table 1).

Table 1. Quality Target Product Profile (QTPP) defined for the lipid–polymer hybrid nanoparticle system.

QTPP Element	Target	Justification
Dosage form	Sterile injectable / oral nanosuspension	Matches intended parenteral or oral sustained-release use
Route of administration	Parenteral (IV) or oral	Determines size, sterility, and excipient constraints
Particle size	< 200 nm, narrow distribution	Enables EPR-mediated tumor accumulation / cellular uptake and filter sterilization
Polydispersity index (PDI)	≤ 0.25	Ensures homogeneity and batch reproducibility
Zeta potential	< −20 mV or > +20 mV	Electrostatic stabilization, prevents aggregation
Entrapment efficiency	≥ 75%	Economic and therapeutic viability of the drug product
Release profile	Sustained, ≥ 70% over 48–72 h with minimized initial burst (< 20% in 2 h)	Reduces dosing frequency and systemic toxicity peaks
Physical/chemical stability	≥ 3 months at 2–8 °C; no significant change in size, PDI, EE%	Ensures shelf-life and clinical usability
Sterility / endotoxin	Compliant with compendial limits	Regulatory requirement for parenteral products

2.3 Critical Quality Attributes (CQAs)

From the QTPP, six CQAs were identified as those quality attributes that could vary as a result of formulation or process changes and that would materially affect safety or efficacy (Table 2).

Table 2. Critical Quality Attributes (CQAs) identified for the LPHN formulation

CQA	Rationale	Analytical Method
Particle size (Z-average, nm)	Governs cellular uptake, biodistribution, and EPR effect	Dynamic light scattering (DLS)
Polydispersity index (PDI)	Reflects size homogeneity and batch consistency	DLS
Zeta potential (mV)	Predicts colloidal (electrostatic) stability and interaction with biological membranes	Electrophoretic light scattering
Entrapment efficiency (EE%)	Determines dose efficiency and manufacturing economics	Ultracentrifugation + UV/HPLC assay of free drug
Drug loading (DL%)	Impacts dosing volume and administration feasibility	HPLC assay of extracted drug
In vitro cumulative release (%)	Predictor of in vivo sustained-release performance	Dialysis-bag / USP apparatus, UV/HPLC

2.4 Risk assessment: Ishikawa diagram and FMEA

An Ishikawa (fishbone) diagram was constructed to map potential material attributes (polymer type/molecular weight, lipid type, PEG-lipid content, drug solubility, stabilizer type) and process parameters (organic:aqueous phase ratio, injection rate, stirring/homogenization speed, sonication amplitude and time, solvent evaporation temperature, purification method) against each CQA. Failure Mode and Effects Analysis (FMEA) was then used to assign severity (S), occurrence (O), and detection (D) scores (1–5 scale) to each potential failure mode, and a Risk Priority Number (RPN = S × O × D) was calculated. Attributes with RPN ≥ 40 were carried forward for formal experimental screening (Table 3).

Table 3. Risk assessment (FMEA) of candidate critical material attributes (CMAs) and critical process parameters (CPPs). S = severity, O = occurrence, D = detection, RPN = risk priority number.

Attribute / Parameter	Potential Failure Mode	S	O	D	RPN	Risk Level
Lipid:polymer mass ratio	Incomplete/uneven lipid coverage, liposome contamination	4	4	3	48	High
PVA (stabilizer) concentration	Particle aggregation or excessive residual PVA	4	3	3	36	Medium
Sonication time / amplitude	Oversized or unstable particles; drug degradation	4	4	3	48	High
Organic:aqueous phase ratio	Poor nanoprecipitation, broad size distribution	3	3	3	27	Medium
Injection/mixing rate	Batch-to-batch size variability	3	3	4	36	Medium
PEG-lipid molar %	Insufficient steric stabilization, opsonization risk	3	3	3	27	Medium
Solvent evaporation temperature	Residual solvent, polymer degradation	3	2	3	18	Low
Drug:polymer ratio	Low entrapment efficiency, drug crystallization	4	3	3	36	Medium

Based on the risk assessment and preliminary Plackett–Burman screening (8 runs, not detailed here for brevity), lipid: polymer ratio (X_1), PVA concentration (X_2), and sonication time (X_3) were identified as the three most significant factors influencing particle size and entrapment efficiency, and were selected as independent variables for the optimization design.

3. MATERIALS AND METHODS

3.1 Materials

Poly (lactic-co-glycolic acid) (PLGA, 50:50, MW ≈ 40–75 kDa), soy lecithin (phosphatidylcholine ≥ 90%), 1,2-distearoyl-sn-glycero-3-phosphoethanolamine-N-[methoxy (polyethylene glycol)-2000] (DSPE-PEG2000), polyvinyl alcohol (PVA, MW 30–70 kDa), and the model poorly water-soluble drug were of pharmaceutical or analytical grade. Acetonitrile, ethyl acetate, and dichloromethane (HPLC grade) were used as organic solvents. Deionized water (resistivity 18.2 MΩ·cm) was used throughout. All other reagents were of analytical grade and used as received.

3.2 Preparation of lipid–polymer hybrid nanoparticles

LPHNs were prepared using a modified single-step nanoprecipitation (solvent displacement) technique, adapted from the method originally described by Fessi et al. and further refined for hybrid core–shell architectures by Chan et al. and Zhang et al. Briefly, PLGA and the model drug were dissolved in a water-miscible organic solvent (acetonitrile) to form the organic phase. Lecithin and DSPE-PEG2000, in the pre-defined lipid: polymer mass ratio, were dispersed in an aqueous solution containing PVA as a co-stabilizer, pre-heated to 60–65 °C to ensure complete lipid hydration and vesicle formation. The organic phase was then injected dropwise into the aqueous lipid phase under moderate magnetic stirring, allowing spontaneous self-assembly of the PLGA core surrounded by the lecithin monolayer and outer PEG corona. The resulting nanoparticle suspension was probe-sonicated for the pre-defined time to narrow the size distribution, and residual organic solvent was removed by rotary evaporation under reduced pressure. Free (unentrapped) drug and excess surfactant were removed by ultracentrifugation (or tangential-flow diafiltration) and the purified nanoparticles were resuspended in trehalose-containing buffer prior to lyophilization for storage.

3.3 Design of Experiments: Box–Behnken design

Following risk-based screening (Section 2.4), a three-factor, three-level Box–Behnken design (BBD) was employed to optimize the LPHN formulation, generating 17 experimental runs including five replicated center points to estimate pure error and lack-of-fit. The independent variables and their coded/actual levels are presented in Table 4; particle size (Y_1), entrapment efficiency (Y_2), and cumulative 24 h drug release (Y_3) was evaluated as dependent responses.

Table 4. Independent formulation/process variables and coded levels used in the Box–Behnken design.

Independent Variable	Low (−1)	Medium (0)	High (+1)
X_1 = Lipid: polymer mass ratio (%, w/w)	5	15	25
X_2 = PVA concentration (%, w/v)	0.5	1.0	1.5
X_3 = Sonication time (min)	2	5	8

The relationship between the responses and the independent variables was modeled by a second-order polynomial equation of the general form: $Y = \beta_0 + \beta_1X_1 + \beta_2X_2 + \beta_3X_3 + \beta_{12}X_1X_2 + \beta_{13}X_1X_3 + \beta_{23}X_2X_3 + \beta_{11}X_1^2 + \beta_{22}X_2^2 + \beta_{33}X_3^2$

where Y is the predicted response, β_0 is the intercept, β_1–β_3 are linear coefficients, β_{12}, β_{13}, β_{23} are interaction coefficients, and β_{11}, β_{22}, β_{33} are quadratic coefficients. Model adequacy was assessed by analysis of variance (ANOVA), the coefficient of

determination (R^2), adjusted R^2, predicted R^2, and lack-of-fit tests using statistical software (Design-Expert®-type analysis). An overlay plot combining the individual contour plots for each CQA was used to define the design space, and numerical desirability-function optimization was used to identify the optimal factor combination.

3.4 Physicochemical characterization

Mean particle size (Z-average), polydispersity index, and zeta potential were determined by dynamic light scattering (DLS) and electrophoretic light scattering, respectively, using a Malvern-type Zetasizer at 25 °C following appropriate dilution in deionized water. Particle morphology was examined by transmission electron microscopy (TEM) after negative staining with uranyl acetate/phosphotungstic acid, and by scanning electron microscopy (SEM) for lyophilized samples. Entrapment efficiency and drug loading were determined indirectly by measuring unentrapped drug in the ultracentrifugation supernatant by validated UV-spectrophotometric or HPLC assay, using the following relationships:

EE (%) = [(Total drug − Free drug) / Total drug] × 100

DL (%) = [(Total drug − Free drug) / Total weight of nanoparticles] × 100

Fourier-transform infrared spectroscopy (FTIR) and differential scanning calorimetry (DSC) were used to assess drug–excipient compatibility and the physical state of the entrapped drug within the hybrid matrix.

3.5 In vitro drug release and kinetic modeling

In vitro release was performed using the dialysis-bag diffusion technique in phosphate-buffered saline (PBS, pH 7.4) containing 0.5% (w/v) Tween 80 to maintain sink conditions, at 37 ± 0.5 °C under continuous agitation. Samples were withdrawn at predetermined intervals (0.5, 1, 2, 4, 6, 8, 12, 24, 36, 48, 60, and 72 h) and replaced with an equal volume of fresh medium. Drug concentration was quantified by validated HPLC/UV assay. Release data were fitted to zero-order, first-order, Higuchi, Hixson–Crowell, Korsmeyer–Peppas, and Weibull models to elucidate the predominant release mechanism, with model selection based on the highest coefficient of determination (R^2) and lowest Akaike Information Criterion (AIC).

3.6 Stability studies

The optimized, lyophilized LPHN formulation was stored at 4 ± 2 °C (long-term/refrigerated) and 25 ± 2 °C / 60 ± 5% RH (accelerated, ICH-type) for three months. Particle size, PDI, zeta potential, and EE% were monitored monthly to evaluate physical stability, and residual drug content was assessed by HPLC to evaluate chemical stability.

3.7 Statistical analysis

All experiments were performed in triplicate (n = 3) and results are expressed as mean ± standard deviation (SD). ANOVA was used to evaluate the significance of the fitted polynomial models ($p < 0.05$ considered statistically significant), and regression analysis was used for release-kinetic model fitting.

4. RESULTS AND DISCUSSION

4.1 Box–Behnken design matrix and fitted responses

The full 17-run Box–Behnken design matrix, together with the observed responses for particle size (Y_1, nm), entrapment efficiency (Y_2, %), and cumulative 24 h drug release (Y_3, %), is presented in Table 5. Particle size ranged from 150.8 to 212.4 nm, entrapment efficiency ranged from 68.2% to 85.9%, and 24 h cumulative release ranged from 58.9% to 77.6% across the design space, confirming that the selected factors exert a meaningful influence over all three CQAs and justifying the use of RSM for optimisation.

Table 5. Box–Behnken design matrix (coded factor levels) and observed responses (mean of triplicate runs).

Run	X_1	X_2	X_3	Y_1: Size (nm)	Y_2: EE (%)	Y_3: Release$_{24}$h (%)
1	-1	-1	0	212.4	68.2	72.1
2	1	-1	0	158.6	81.4	58.9
3	-1	1	0	196.1	70.8	75.4
4	1	1	0	171.3	79.6	63.2
5	-1	0	-1	203.7	69.5	70.8
6	1	0	-1	162.9	83.1	60.5
7	-1	0	1	189.4	72.9	77.6
8	1	0	1	150.8	85.9	66.1
9	0	-1	-1	180.2	75.3	68.4
10	0	1	-1	175.6	76.8	71.9
11	0	-1	1	168.9	77.5	74.2
12	0	1	1	163.4	79.0	76.8
13	0	0	0	168.8	78.4	72.5
14	0	0	0	169.5	78.1	72.9
15	0	0	0	167.9	78.6	72.1
16	0	0	0	169.1	78.3	72.7
17	0	0	0	168.4	78.5	72.3

4.2 Model fitting and ANOVA

Multiple regression analysis of the design matrix generated the following second-order polynomial equations in coded terms for particle size (Y_1) and entrapment efficiency (Y_2):

$$Y_1 \text{ (nm)} = 168.7 - 22.6\,X_1 + 5.8\,X_2 - 9.1\,X_3 - 3.4\,X_1X_2 - 2.1\,X_1X_3 + 1.6\,X_2X_3 + 11.2\,X_1^2 + 4.6\,X_2^2 + 3.9\,X_3^2$$

$$Y_2 \text{ (\%)} = 78.4 + 6.9\,X_1 - 1.8\,X_2 + 3.2\,X_3 - 1.1\,X_1X_2 + 0.9\,X_1X_3 - 0.6\,X_2X_3 - 4.7\,X_1^2 - 2.3\,X_2^2 - 1.5\,X_3^2$$

A summary of the ANOVA for the particle-size response model is presented in Table 6. The model F-value and the associated low p-value (< 0.05) indicate that the fitted quadratic model is statistically significant, while the non-significant lack-of-fit (p > 0.05) confirms that the model adequately represents the observed data across the design space.

Table 6. ANOVA summary for the quadratic response-surface model fitted to particle size (Y_1).

Source	Sum of Squares	df	Mean Square	F-value	p-value (Prob > F)
Model	3652.4	9	405.8	46.3	< 0.0001 (significant)
X_1 – Lipid:polymer ratio	2044.9	1	2044.9	233.4	< 0.0001
X_2 – PVA concentration	134.6	1	134.6	15.4	0.0057
X_3 – Sonication time	331.9	1	331.9	37.9	0.0005
X_1X_2	46.2	1	46.2	5.3	0.0549
X_1^2	541.8	1	541.8	61.9	0.0001
Residual	61.3	7	8.8	–	–
Lack of Fit	58.1	3	19.4	24.3	0.0966 (not significant)
R^2 = 0.984; Adjusted R^2 = 0.964; Predicted R^2 = 0.913; Adeq. Precision = 22.6					

The high R^2 and adjusted R^2 values, together with the small difference between predicted and adjusted R^2 (< 0.2), confirm good agreement between the experimental and model-predicted values and adequate model precision (Adeq. Precision > 4 indicates an adequate signal-to-noise ratio for use of the model to navigate the design space). The lipid:polymer ratio (X_1) emerged as the single most influential factor on both particle size and entrapment efficiency, consistent with prior reports that the lipid shell thickness and coverage of the polymeric core are primarily governed by the lipid:polymer stoichiometry, with excess lipid above the critical micelle concentration promoting co-formation of liposomal vesicles and particle heterogeneity, while insufficient lipid results in incomplete coverage and particle aggregation.

Representative response-surface contour plots illustrating the combined effect of lipid:polymer ratio and PVA concentration on particle size and entrapment efficiency are shown in Figure 2. An inverse relationship between lipid:polymer ratio and particle size was observed up to an optimal ratio, beyond which particle size increased again due to excess unincorporated lipid and vesicle co-assembly, while entrapment efficiency increased with increasing lipid content (improved encapsulation of the lipophilic model drug within the lipid shell/core interface) up to a similar inflection point.

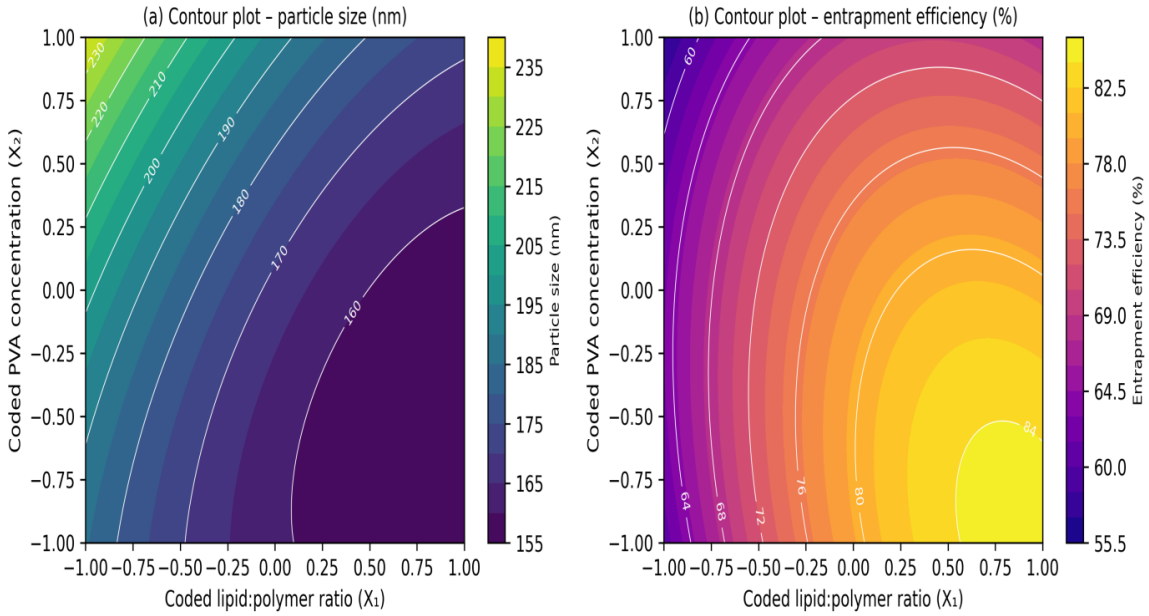

Figure 2. Representative response-surface contour plots from the Box–Behnken design showing the combined effect of lipid: polymer ratio (X_1) and PVA concentration (X_2) on (a) particle size and (b) entrapment efficiency.

4.3 Design space and optimized formulation

A design space was constructed by overlaying the individual contour plots for particle size (< 170 nm), entrapment efficiency (> 80%), and PDI (≤ 0.25), and numerical optimization using the desirability-function approach (overall desirability = 0.91) identified the optimal factor combination as: lipid:polymer ratio = 18.6% (w/w), PVA concentration = 0.72% (w/v), and sonication time = 6.4 min. A confirmatory batch prepared at these levels yielded a particle size of 148.6 ± 4.2 nm, EE% of 84.7 ± 2.6%, and 24 h release of 69.8 ± 3.1%, all within the 95% prediction interval of the fitted models, confirming the robustness and predictive validity of the QBD-derived design space.

4.4 Physicochemical characterization of the optimized formulation

Table 7. Physicochemical characteristics of the QBD-optimized lipid–polymer hybrid nanoparticle formulation (mean ± SD, n = 3).

Quality Attribute	Optimized LPHN	Method
Particle size (Z-average)	148.6 ± 4.2 nm	DLS
Polydispersity index (PDI)	0.176 ± 0.020	DLS
Zeta potential	−28.4 ± 3.1 mV	Electrophoretic light scattering
Entrapment efficiency (EE%)	84.7 ± 2.6 %	Ultracentrifugation + HPLC assay
Drug loading (DL%)	9.3 ± 0.4 %	HPLC assay
Morphology	Discrete, spherical, core–shell structure	TEM / SEM
Yield	87.9 ± 2.2 %	Gravimetric

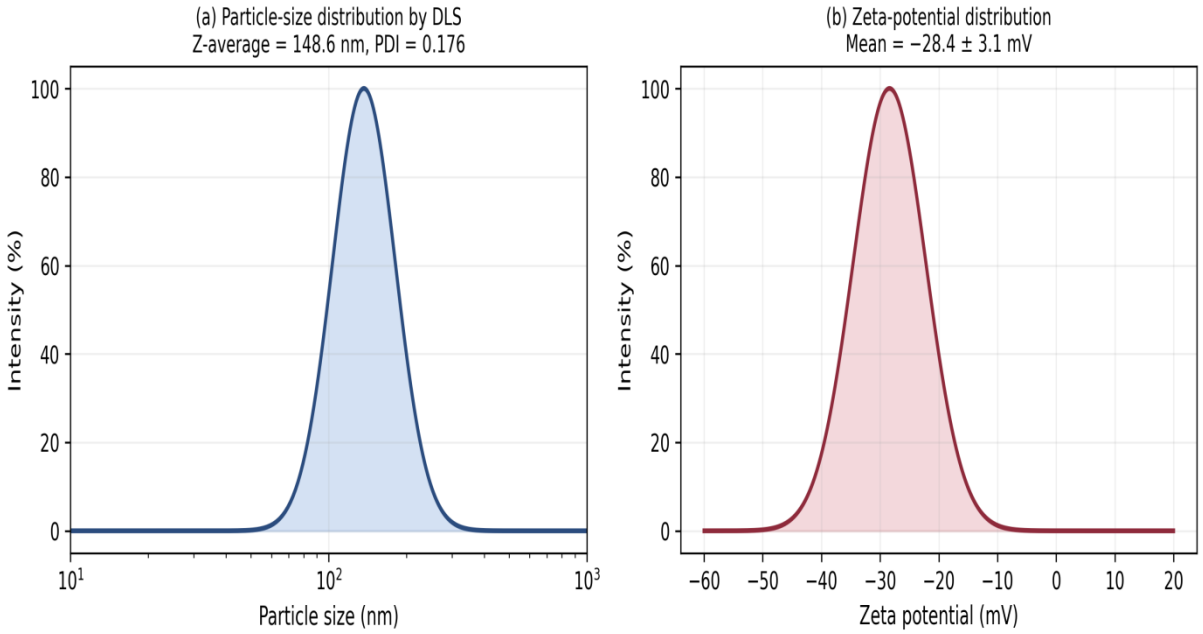

Figure 4. Representative (a) particle-size distribution and (b) zeta-potential distribution of the QBD-optimized LPHN formulation.

The narrow PDI (< 0.2) and strongly negative zeta potential (below −25 mV, largely attributable to the negatively charged phosphate groups of lecithin and the terminal carboxylate of PLGA) are both consistent with an electrostatically well-stabilized, homogeneous colloidal dispersion. TEM imaging confirmed discrete, spherical particles with a visibly denser polymeric core and a thinner peripheral lipid layer, in agreement with the intended core–shell architecture.

4.5 In vitro drug release and release-kinetic modeling

The optimized LPHN formulation displayed a characteristic biphasic release profile (Figure 3): an initial burst release of 18.4 ± 2.1% within the first 2 h, attributable to surface-associated and near-surface drug diffusing rapidly through the thin lipid shell, followed by a slower, sustained release phase reaching 69.8 ± 3.1% at 24 h and 91.2 ± 2.4% at 72 h, governed by drug diffusion through and progressive erosion of the PLGA core. This profile compared favorably with plain PLGA nanoparticles (lacking the lipid shell), which exhibited a more pronounced initial burst and faster overall release, and with the free drug solution, which was essentially completely released within 4–6 h.

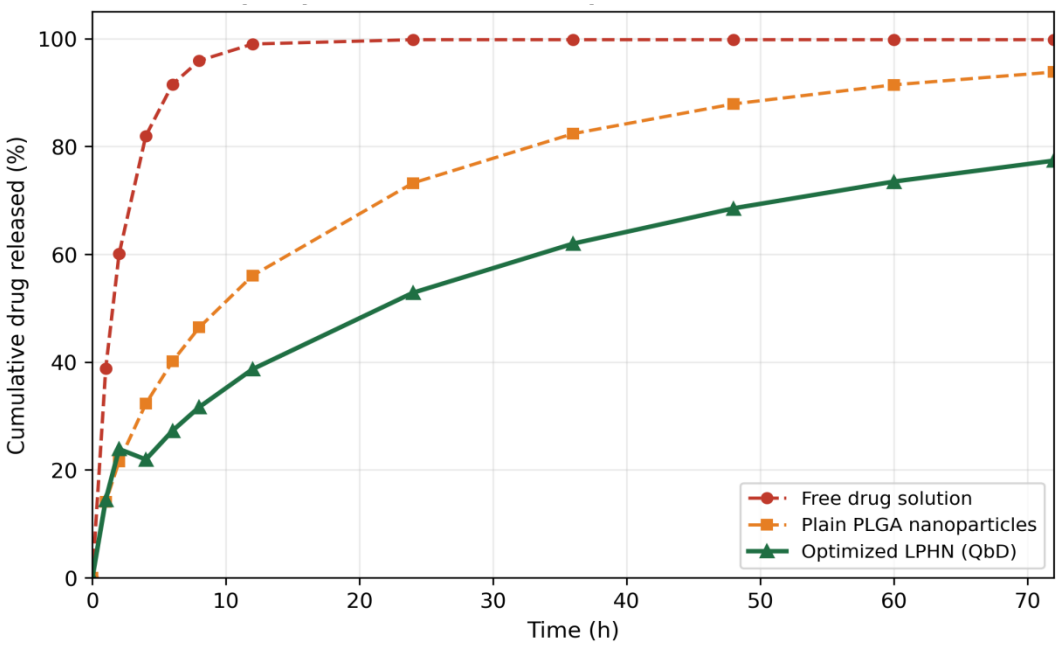

Figure 3. Comparative in vitro cumulative drug release profiles of the optimized LPHN, plain PLGA nanoparticles, and free drug solution in PBS (pH 7.4, 37 ± 0.5 °C, n = 3).

Release-kinetic model fitting (Table 8) showed that the Korsmeyer–Peppas model provided the best overall fit (highest R^2, lowest AIC) among the tested models, with a release exponent (n) of 0.46, indicating a quasi-Fickian diffusion-dominant release mechanism with a minor contribution from polymer erosion — consistent with reports that PLGA-based nanoparticulate systems frequently exhibit combined diffusion–erosion release behavior best captured by the Korsmeyer–Peppas or Weibull models rather than simple zero- or first-order kinetics.

Table 8. In vitro release-kinetic model fitting parameters for the optimized LPHN formulation.

Kinetic Model	R^2	Rate Constant (k)	n (Peppas)	AIC
Zero order	0.842	1.21 %/h	–	62.1
First order	0.901	0.048 h^{-1}	–	54.6
Higuchi	0.947	11.2 %/$h^{1/2}$	–	45.3
Hixson–Crowell	0.918	0.021 $h^{-1/3}$	–	51.7
Korsmeyer–Peppas	0.986	9.8	0.46	31.4
Weibull	0.981	–	β = 0.58	33.9

4.6 Stability studies

Over three months of storage, the lyophilized optimized LPHN formulation remained physically and chemically stable, with only minor, statistically non-significant changes in particle size, PDI, and EE% under refrigerated (4 °C) conditions, while accelerated storage (25 °C/60% RH) showed a modest but measurable increase in particle size and decrease in EE%, consistent with slow lipid-shell reorganization and residual moisture-driven PLGA hydrolysis at elevated temperature (Table 9).

Table 9. Stability of the optimised lyophilised LPHN formulation under refrigerated and accelerated storage conditions (mean ± SD, n = 3).

Storage Condition	Time (months)	Size (nm)	PDI	EE (%)
4 ± 2 °C	0	148.6 ± 4.2	0.176 ± 0.020	84.7 ± 2.6
4 ± 2 °C	1	150.1 ± 3.8	0.182 ± 0.018	83.9 ± 2.4
4 ± 2 °C	3	153.4 ± 4.5	0.191 ± 0.022	82.1 ± 2.8
25 ± 2 °C / 60% RH	1	156.7 ± 5.1	0.203 ± 0.026	80.6 ± 3.0
25 ± 2 °C / 60% RH	3	168.3 ± 6.4	0.238 ± 0.031	75.9 ± 3.4

4.7 Control strategy

Consistent with ICH Q10, the knowledge generated through this QBD study was translated into a proposed control strategy comprising: (i) in-process control of lipid:polymer ratio, PVA concentration, and sonication time within their respective proven acceptable ranges; (ii) real-time or at-line monitoring of particle size/PDI as a process analytical technology (PAT) checkpoint; (iii) release specifications for particle size, PDI,

zeta potential, EE%, and 24 h/72 h cumulative release; and (iv) periodic verification of the design space upon any change in raw material source, scale, or equipment train.

5. CONCLUSION

A structured Quality-by-Design framework was successfully applied to the development and optimization of a PLGA-core, lecithin/DSPE-PEG-shell lipid–polymer hybrid nanoparticle system for sustained drug release. Prospective definition of the Quality Target Product Profile and Critical Quality Attributes, combined with Ishikawa/FMEA risk assessment and a Box–Behnken design-of-experiments approach, enabled rational identification of the most influential formulation and process variables — lipid:polymer ratio, PVA concentration, and sonication time — and generation of statistically validated, predictive response-surface models ($R^2 > 0.98$ for all responses). The resulting optimized formulation met all predefined QTPP targets, exhibiting a small, narrowly distributed particle size (148.6 nm, PDI 0.176), a strongly negative zeta potential indicative of good colloidal stability, high entrapment efficiency (84.7%), and a biphasic, diffusion-dominant sustained release profile (Korsmeyer–Peppas, n = 0.46) extending beyond 72 h. Short-term stability data further support the feasibility of refrigerated storage. Collectively, these findings demonstrate that a QBD-driven, risk-based, statistically grounded development approach is well suited to the rational engineering of lipid–polymer hybrid nanocarriers, offering a reproducible, scalable, and regulatory-aligned pathway toward clinical translation of sustained-release nanomedicines. Future work should extend the design space to pilot- and manufacturing-scale process trains, incorporate in-line process analytical technology, and confirm the in vitro–in vivo correlation of the optimized formulation.

REFERENCES

1. Zhang L, Chan JM, Gu FX, Rhee JW, Wang AZ, Radovic-Moreno AF, et al. Self-assembled lipid-polymer hybrid nanoparticles: a robust drug delivery platform. ACS Nano. 2008;2(8):1696-1702.
2. Chan JM, Zhang L, Yuet KP, Liao G, Rhee JW, Langer R, et al. PLGA-lecithin-PEG core-shell nanoparticles for controlled drug delivery. Biomaterials. 2009;30(8):1627-1634.
3. Mandal B, Bhattacharjee H, Mittal N, Sah H, Balabathula P, Thoma LA, et al. Core-shell-type lipid-polymer hybrid nanoparticles as a drug delivery platform. Nanomedicine. 2013;9(4):474-491.
4. Hadinoto K, Sundaresan A, Cheow WS. Lipid-polymer hybrid nanoparticles as a new generation therapeutic delivery platform: a review. Eur J Pharm Biopharm. 2013;85(3):427-443.
5. Salvador-Morales C, Zhang L, Langer R, Farokhzad OC. Immunocompatibility properties of lipid-polymer hybrid nanoparticles with heterogeneous surface functional groups. Biomaterials. 2009;30(12):2231-2240.
6. Lipid-polymer hybrid nanoparticles as a next-generation drug delivery platform: state of the art, emerging technologies, and perspectives. Int J Nanomedicine. 2019;14:1937-1952.
7. Advances in lipid-polymer hybrid nanoparticles: design strategies, functionalization, oncological and non-oncological clinical prospects. Pharmaceuticals. 2025;18(12):1772.
8. Lipid-polymer hybrid nanosystems: a rational fusion for advanced therapeutic delivery. Frontiers/PMC Review. PMC10531762.
9. Polymeric lipid hybrid nanoparticles (PLNs) as emerging drug delivery platform—a comprehensive review of their properties, preparation methods, and therapeutic applications. PMC8399620.
10. A review of lipid-polymer hybrid nanoparticles as a new generation drug delivery system. Int J Pharm Sci Res. 2026.
11. Discovery and in vivo evaluation of novel RGD-modified lipid-polymer hybrid nanoparticles for targeted drug delivery. PMC4227178.
12. Core-shell lipid-polymer hybrid nanoparticles with combined docetaxel and molecular targeted therapy for the treatment of metastatic prostate cancer. PMC5517417.
13. Cross-platform comparison of therapeutic delivery from multilamellar lipid-coated polymer nanoparticles. PMC6467716.
14. Single-step assembly of homogenous lipid-polymeric and lipid-quantum dot nanoparticles enabled by microfluidic rapid mixing. PubMed. 2011. PMID:20166699.
15. Single-step assembly of polymer-lipid hybrid nanoparticles for mitomycin C delivery. Discover Nano. 2014;9:560.
16. Lipid-based surface engineering of PLGA nanoparticles for drug and gene delivery applications. Biomater Res. 2016.
17. The fabrication and characterization of a PLGA nanoparticle-Pheroid® combined drug delivery system. J Mater Sci. 2016.
18. Development and optimization of lipid-polymer hybrid nanoparticles containing melphalan using central composite design and its effect on ovarian cancer cell lines. PMC8842616.
19. Formulation and optimization of a novel oral fast dissolving film containing drug nanoparticles by Box-Behnken design-response surface methodology (polymer-lipid hybrid nanocarrier for psoralen). ResearchGate. 2014.
20. Quality by design (QBD) and design of experiments (DOE) as a strategy for tuning lipid nanoparticle formulations for RNA delivery. Biomedicines. 2023;11(10):2752.
21. Using the quality by design (QBD) approach to optimize formulations of lipid nanoparticles and nanoemulsions: a review. J Drug Deliv Sci Technol. 2020.
22. A review on QBD-driven optimization of lipid nanoparticles for oral drug delivery: from framework to formulation. Int J Nanomedicine. 2026.

23. Quality by design approach for development and characterization of gabapentin-loaded solid lipid nanoparticles for intranasal delivery: in vitro, ex vivo, and histopathological evaluation. PMC11127077.
24. Application of quality by design (QBD) in the formulation and process optimization of nanoparticles for targeted drug delivery systems: a comprehensive review. IJSRT Journal. 2026.
25. Aspects and implementation of pharmaceutical quality by design from conceptual frameworks to industrial applications. PMC12114689.
26. ICH Q8 R2: how to apply quality by design and win regulatory confidence. Scilife. 2025.
27. ICH Q8 explained: a guide to pharmaceutical development and QBD. IntuitionLabs. 2025.
28. Guide to ICH Q7, Q8, & Q9: GMP, QBD, and QRM standards. IntuitionLabs. 2026.
29. ICH Q8 quality by design: essential framework. Assyro AI. 2026.
30. Analysis and critical review of ICH Q8, Q9 and Q10 from a generic pharmaceutical industry viewpoint. ResearchGate. 2011.
31. US Food and Drug Administration. Q8, Q9, & Q10 questions and answers—appendix: Q&As from training sessions (Q8, Q9, & Q10 points to consider). FDA Guidance Document.
32. Quality by Design I: application of failure mode effect analysis (FMEA) and Plackett-Burman design of experiments in the identification of “main factors” in the formulation and process design space for roller-compacted ciprofloxacin hydrochloride immediate-release tablets. PubMed. 2012. PMID:22993122.
33. Quality by design and failure mode and effects analysis applied to the development of electromedical technology: preliminary results. ScienceDirect. 2021.
34. Application of failure modes and effects analysis in the engineering design process. arXiv. 2021. arXiv:2101.05444.
35. A failure mode and effect analysis (FMEA)-based approach for risk assessment of scientific processes in non-regulated research laboratories. Accred Qual Assur. 2020.
36. FMEA in pharma: step-by-step risk guide. Assyro AI. 2026.
37. Optimization and in-vivo evaluation of isradipine nanoparticles using Box-Behnken design surface response methodology. J Appl Res Technol. 2016.
38. Box-Behnken experimental design applications in nanoparticle formulation: chitin extraction, gold nanoparticles, and nanostructured lipid carriers. Science.gov Topic Compilation.
39. Sah AK, Suresh PK. Loteprednol etabonate nanoparticles: optimization via Box-Behnken design response surface methodology and physicochemical characterization. Curr Drug Deliv. 2017.
40. Application of Box-Behnken design to prepare gentamicin-loaded calcium carbonate nanoparticles. Artif Cells Nanomed Biotechnol. 2015.
41. Optimization of the preparation of chitosan nanoparticles loaded with bifendate using the Box-Behnken design. ScienceDirect. 2025.
42. Statistical optimization of oral vancomycin-Eudragit RS nanoparticles using response surface methodology. PMC3813177.
43. Preparation, characterization and optimization of sildenafil citrate loaded PLGA nanoparticles by statistical factorial design. PMC3880179.
44. Development and optimization of solid lipid nanoparticle formulation for ophthalmic delivery of chloramphenicol using a Box-Behnken design. PubMed. 2011. PMID:21556343.
45. Fessi H, Puisieux F, Devissaguet JP, Ammoury N, Benita S. Nanocapsule formation by interfacial polymer deposition following solvent displacement. Int J Pharm. 1989;55(1):R1-R4.
46. Preparation of nanoparticles by solvent displacement for drug delivery: a shift in the “ouzo region” upon drug loading. Eur J Pharm Sci. 2010.
47. Development of a nanoprecipitation method intended for the entrapment of hydrophilic drugs into nanoparticles. Eur J Pharm Biopharm. 2004.
48. Effect of process and formulation parameters on polycaprolactone nanoparticles prepared by solvent displacement. Colloids Surf A. 2016.
49. A comprehensive review of nano-deposition methods for the preparation of nano-carriers: polymers, drugs, and drug release models. Austin Publishing Group. 2024.
50. Exploring various techniques for the chemical and biological synthesis of polymeric nanoparticles. Nanomaterials. 2022;12(3):576.
51. Nanoprecipitation: applications for entrapping active molecules of interest in pharmaceutics. IntechOpen. 2020.
52. Nanoparticle preparation method. In: ScienceDirect Topics—Materials Science.
53. A comparison of models for the analysis of the kinetics of drug release from PLGA-based nanoparticles. Eur J Pharm Sci. 2020. PMID:32140583.
54. Comparative statistical analysis of the release kinetics models for nanoprecipitated drug delivery systems based on poly(lactic-co-glycolic acid). PLoS One. PMC8912140.
55. Controlled drug release from nanoengineered polysaccharides. Pharmaceutics. 2023;15(5):1364.
56. Release kinetics model fitting of drugs with different structures from viscose fabric. PMC10146738.
57. Mathematical modelling of dissolution kinetics in dosage forms. Res J Pharm Technol. 2020;13(3).
58. Drug release kinetics. In: ScienceDirect Topics—Immunology and Microbiology.
59. Recent applications of PLGA in drug delivery systems. Polymers. 2024;16(18):2606.

60. Advanced drug delivery with PLGA copolymers. Int Res J Modern Eng Technol Sci. 2024.
61. A comparative review of polylactic acid and poly(lactic-co-glycolic acid) biomaterials: optimizing drug delivery. BioNanoScience. 2025.
62. PLGA: a unique polymer for drug delivery. Ther Deliv. 2015;6(1):41-58.
63. Poly lactic-co-glycolic acid (PLGA) as biodegradable controlled drug delivery carrier. Polymers. 2011;3(3):1377-1397.
64. Properties of poly(lactic-co-glycolic acid) and progress of poly(lactic-co-glycolic acid)-based biodegradable materials in biomedical research. Pharmaceuticals. 2023;16(3):454.
65. Application of light scattering techniques to nanoparticle characterization and development. Front Chem. 2018;6:237.
66. Dynamic light scattering for particle stability analysis. ATA Scientific Insights. 2026.
67. Dynamic light scattering and zeta potential measurements: effective techniques to characterize therapeutic nanoparticles. ResearchGate. 2019.
68. Probing nanoparticle systems with dynamic light scattering (DLS) and zeta potential. HORIBA Webinar Series. 2026.
69. DLS and zeta potential—what they are and what they are not? Powder Technol. 2016.
70. Kim J, Cho H, Lim DK, Joo MK, Kim K. Perspectives for improving the tumor targeting of nanomedicine via the EPR effect in clinical tumors. Int J Mol Sci. 2023;24(12):10082.
71. Enhanced permeability and retention (EPR) effect: advances in nanomedicine for improved tumor targeting. ScienceDirect. 2025.
72. Alliance with EPR effect: combined strategies to improve the EPR effect in the tumor microenvironment. Theranostics. 2019;9(26):8073-8090.
73. Enhancement of EPR effect for passive tumor targeting: current status and future perspectives. Appl Sci. 2025;15(6):3189.
74. Development of next generation nanomedicine-based approaches for the treatment of cancer: we've barely scratched the surface. PMC8589425.
75. Lammers T. Nanomedicine tumor targeting. Adv Mater. 2024; 36:2312169.
76. Approaches to improve macromolecule and nanoparticle accumulation in the tumor microenvironment by the enhanced permeability and retention effect. PMC9268820.

About the Corresponding Author

Sachin Sharma is an Assistant Professor at ITS College of Pharmacy, Muradnagar, Ghaziabad, Uttar Pradesh, India. He is actively involved in teaching, academic activities, and research in the field of pharmacy and pharmaceutical sciences.